Integrated near infrared and ultraviolet spectroscopy techniques for determination of hydrate inhibitors in the presence of NaCl

INTEGRATED NEAR INFRARED AND ULTRAVIOLET SPECTROSCOPY TECHNIQUES FOR DETERMINATION OF HYDRATE INHIBITORS IN THE PRESENCE OF NACL

Reza K.Haghi[a,b], Jinhai Yang[a,*], Bahman Tohidi[a]

[a]*Hydrates, Flow Assurance & Phase Equilibria Research Group, Institute of Petroleum Engineering, School of Energy, Geoscience, Infrastructure and Society, Heriot-Watt University, Edinburgh EH14 4AS, Scotland, UK*

[b] *James Hutton Institute, Craigiebuckler, Aberdeen AB15 8QH, Scotland, UK*

[*] *Corresponding Author: petjy@hw.ac.uk*

Abstract

Injection of chemical inhibitors is the most widely used method to prevent the formation of gas hydrates in gas transporting pipelines. It is usual that high dosage of hydrate inhibitors has to be applied to minimise the risk of hydrate blockages, which can cause more operation cost and severe environmental damage. Monitoring the concentration of hydrate inhibitors in the pipeline could help the operator to determine the hydrate safety margin accurately therefore optimise inhibitor injection rate (i.e., ensuring adequate inhibition and avoiding over inhibition).

In this study, the application of spectroscopic techniques was investigated to measure the concentration of both thermodynamic and low dosage hydrate inhibitors in water/brine by coupling UV and NIR spectra.Various partial least-squares (PLS) regression models were developed and evaluated at three different spectral regions (1400-1600, 1600-1850 and 1400-1850 nm) to determine the concentration of hydrate inhibitors and NaCl in three different

inhibition systems: a) mono-ethylene glycol (MEG)-NaCl, b) methanol (MeOH)-NaCl and c) Poly-nvinylcaprolactam (PVCap)-MEG-NaCl. The developed PLS models were further evaluated for a typical MEG-NaCl inhibition system by determining the concentration of MEG and NaCl during natural gas hydrate formation and dissociation. The results confirmed that the integrated NIR-UV spectroscopy technique can be used as a simple, quick, and reliable means for monitoring simultaneously the hydrate inhibitors and NaCl in pipelines.

1. INTRODUCTION

Formation of gas hydrates from natural gas and water can lead to blockage in hydrocarbon transportation pipelines, causing extensive damage to the pipelines and potential risk to personnel safety. [1] Currently, different types of hydrate inhibitors are utilized to avoid the formation of gas hydrates in hydrocarbons transport pipelines. Thermodynamic hydrate inhibitors (THIs, i.e., alcohols and glycols) are the most commonly used hydrate inhibitors in the industry since 1930.[2] However, in the last two decades, interest has been shown in using low dosage hydrate inhibitors (LDHIs) such as kinetic hydrate inhibitors (KHIs) and Anti-agglomorents (AAs). LDHIs, as their name implies, are injected in a small quantity (0.5 to 3 mass %)[3] compared to THIs which are injected into a stream of hydrocarbons in high concentration (up to 60 mass%), depending on the operation conditions (i.e., pressure, temperature, and water cut).[4]

There is a risk of hydrate blockage if pressure and temperature conditions are inside the hydrate stability zone Otherwise, the formation of gas hydrate is not expected. Hydrate safety margin is defined as the temperature difference between the actual fluid temperature and the hydrate dissociation temperature at a given pressure.[5] The inhibitor injection rate is normally considered based on worst operating conditions (i.e., maximum pressure and minimum temperature) with a significant safety margin (e.g., 3–5 K outside the hydrate stability zone).

This margin of saftey is normally applied because of the uncertainty in multicomponent gas hydrate equilibrium calculations and lack of information about the actual concentration of salts, inhibitors and gas components in the system. Thus, to predict the hydrate stability zone and calculate the hydrate safety margin according to pipeline operation conditions, it is essential to know the accurate concentration of hydrate inhibitors and salt as well as hydrocarbon compositions. However, we should keep in mind that, in real field application, unexpected issues such as a change in the concentration of produced water, human error, equipment breakdown, etc., could also affect the actual concentration of hydrate inhibitors.[1] Thus, monitoring the concentration of hydrate inhibitors in the pipeline can assist the operator to determine the hydrate safety margin accurately, which would result in optimising inhibitor injection rate. The main goal of this study is to develop a new method by coupling the UV (ultraviolet) and NIR (near infrared) spectra for optimising inhibitor injection.

Several studies were reported to measure the concentration of THIs, KHIs and salt in aqueous solutions. Henning et al.[6] reported the use of an acoustic multi-sensor for measuring the concentration of alcohols such as MeOH and ethanol (EtOH) in aqueous solutions in the absence of salt. Sandengen et al.[7] provided an equation to calculate the concentration of salt and MEG by measuring the conductivity and density of the water sample at a temperature of 298.15 K and 293.15 K respectively. Based on their results, the accuracy of the calculated MEG concentration was within ± 2 mass %, whereas an estimated accuracy of 5 to 6% was reported for NaCl. In 2013, a new hydrate inhibition monitoring/optimising system called conductivity-velocity (C-V) method were developed by Yang et al.[8] An artificial neural network model (ANN) was created utilising the measured conductivity and velocity data and used to determine the concentration of THI or KHI and NaCl in aqueous solutions.

Near-infrared (NIR) spectroscopy was also successfully applied measure the concentration of salt in water samples. Though it is known that salt does not absorb NIR light, the presence of

salt in the water sample can cause an alteration in the structure of water by perturbation of the hydrogen bond network which results in an overall change in the measured spectrum [9]. This phenomenon was used by researchers to monitor and measure the concentration of different types of salt in water. In 1993, Lin et al. [10] determined the concentration of salt (up to 35 mass%) in seawater by employing NIR spectroscopy. They used the range between 1100 to 1900 nm for the construction of the calibration models. The accuracy of the measurement was believed to be within 0.22%. Grant et al.[11] also used NIR spectroscopic technique to measure the concentration of NaOH, Na_2CO_3 and NaCl in aqueous solutions in a range of concentrations from 0 to 15 mass%. In another study that carried out by Gowen et al.[9], they revealed that NIR spectroscopy is capable of determining low concentrations of different types of salt (i.e., NaCl, KCl, $MgCl_2$ and $AlCl_3$) in the order of 1000 ppm in solutions containing water and salt. They selected the spectral range from 1300 to 1600 nm as the final range for developing of the partial least square regression model as it provides lower error values for the prediction data set. Moreover, vibrational spectroscopy methods such as NIR and UV spectroscopy can provide information about the evolution of KHIs and THIs contents in various fluid systems. Several studies were carried out to measure the concentration of EtOH and MeOH in gasoline by combining NIR and chemometric methods.[12-14]

Poly-nvinylcaprolactam (PVCap hereafter) is a low molecular weight polymer and recognized as a KHI which has recently become increasingly popular. Anderson et al.[15] utilised a UV-visible spectrometer to detect the concentration of PVCAp in water. They reported a detection limit of PVCap in the order of about 0.003 mass% in a solution containing PVcap and distilled water. Gibsson *et al*.[16] utilised a UV-Vis spectrometer to measure the concentration of various types of polymers in deionized water. They could detect the concentration of different polymers in water samples with a detection limit of 0.5 ppm using single wavelength calibration in the ranges 200-220 nm.

In recent years, the oil and gas industry moving toward deep water conditions requires deployment of combined a KHI with a THI to reduce both subcooling that always limits the performance of KHIs and the required volume of thermodynamic.[17, 18] For example, recent studies have shown that it is possible to obtain synergistic kinetic inhibition by mixing specific amount of PVCap and MEG in the aqueous phase of multi-component natural gas systems.[19, 20] Thus, monitoring the concentration of both THIs and KHIs hydrate inhibitors hase become necessary to improve the reliability of the hybrid hydrate inhibition strategy.

To our knowledge, there are no such means that can quantify the concentration of THIs, KHIs and NaCl simultaneously. In this work, we investigated the potential of NIR and UV spectroscopic methods associated with partial least square (PLS) method to predict the concentration of MEG, MeOH, PVCap in the absence and presence of NaCl in aqueous solutions.

2. SPECTROSCOPY TECHNIQUE

2.1 Absorbance spectra of water, MEG, MeOH, and PVCap

Vibrational spectroscopic techniques are attractive technologies for measuring the concentration of chemical species in fluid samples because they are non-invasive/destructive, typically offer fast response times, minimum sample preparation, and minimum sample volume is required, and the modern instrumentation has a minimum footprint. In comparison, other conventional methods, for example, gas chromatography (GC), colourimetric and gravimetric methods, are time-consuming, require a high degree of analytical skills, and have large footprints that are not amenable to developing portable analytical instruments. Utilizing the NIR region of the spectrum (780 to 2500 nm) offers the ability to discriminate absorption features of organic species (e.g. alcohols) from those of water, which is a very strong absorber across the majority of the infrared spectrum (Figure 1). It is apparent that molecules of water

absorb the NIR light strongly at two different regions. In Figure 1, the NIR response from water across the wavelength region of 1000 - 2100 nm, noting the main features at approx. 1450 and 1900 nm, which correspond to the first overtone and combination bands of O-H bonds, respectively. The solvated salt ions, specifically Na^+ and Cl^-, are themselves transparent to the infrared light. However, the presence of salt in the water sample can cause an alteration in the structure of water by perturbation of the hydrogen bond network in the combination and overtone regions which results in an overall change in the measured spectrum. The extent of these perturbations depends upon the properties of the solute, such as size and ionic strength. These changes can be detected in the measured spectra and hence used to determine the concentration of salt in water samples. MeOH and MEG absorb the NIR light in the NIR region, according to the structure of their molecules. MeOH molecules contain one methyl group (-CH_3) and one hydroxyl group (-OH), whereas MEG molecules have two methylene groups (-CH_2) and two hydroxyl groups. The NIR spectra of pure MeOH, pure MEG and deionized water in the range of 1000 to 2200 nm are shown in Figure 1. The absorption bands in the range between 1450 and 1600 nm are related to the first overtone of O-H bond, while the absorption bands between 1600 to 1900 nm belong to first overtones of the CH_3 (methyl) and CH_2 (methylene) groups. It is clear that there are some interferences between spectra of alcohols (MeOH and MEG) and water in almost the NIR entire region. To overcome this problem, and extract the desired information from the collected spectra, the capability of partial least square (PLS) calibration models were investigated in different spectral ranges between 1400 to1850 nm. The ranges higher than 1850 nm were excluded from the analysis due to very high absorption of water which produced large errors on MeOH and MEG predictions. In the region comprised between 1000 and 1400 nm the spectra of the water, MEG and MeOH do not show any particular absorption feature, and they were removed from the dataset (See Figure 2).

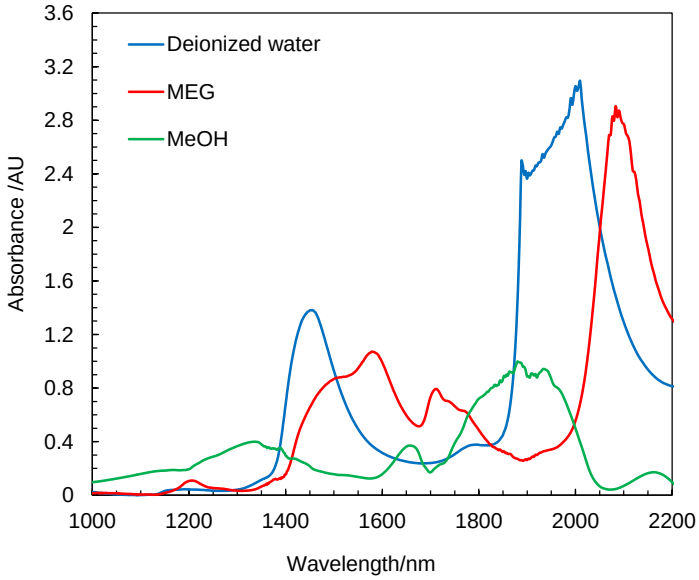

Figure 1. FTNIR Spectra of pure water, MeOH and MEG, captured by the FTNIR spectrometer at atmospheric pressure and 293.15 K with an effective path-length of 1mm .

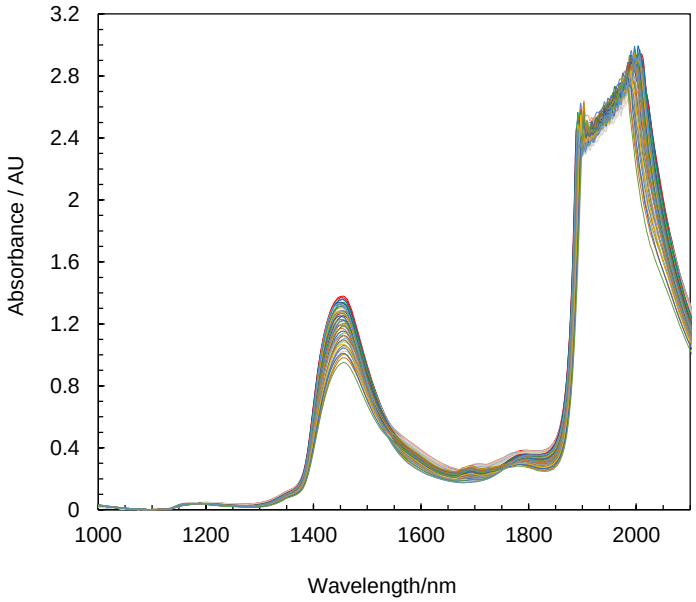

Figure 2. NIR Spectra of 50 water samples with different MEG, MeOH and salt concentrations

UV region can provide some valuable information regarding the evolution of polymer contents in aqueous solutions. It was noticed that the absorbance value increases significantly between around 300 and 400 nm while the concentration of PVCap in deionized water varies from 0.5 to 3 mass% (See Figure 3). A linear relationship was observed between the concentration of

PVCap and absorbance. In this study, the NIR region was employed to determine the concentration of NaCl, MEG, and MeOH, whereas UV region was utilised to detect the changes in the concentration of PVCap.

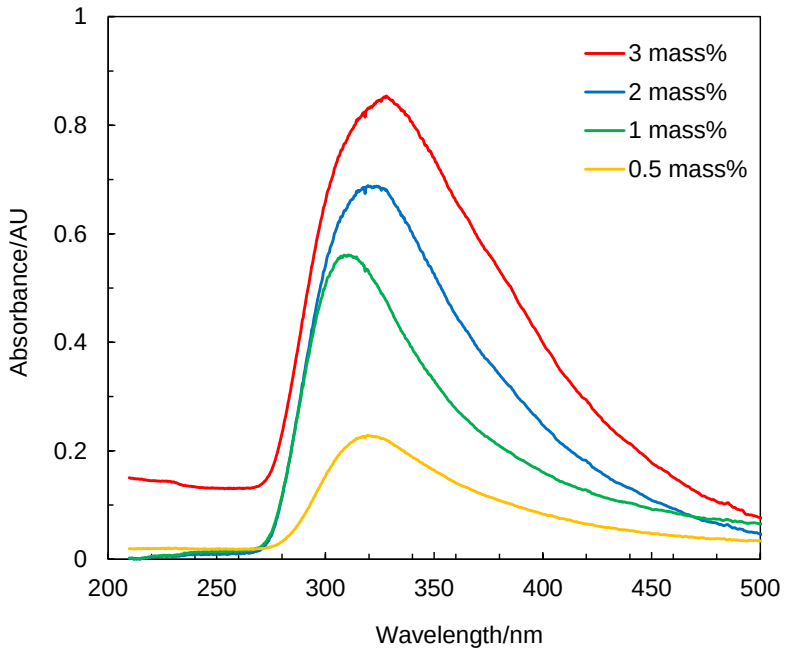

Figure 3. UV spectra of solutions with various PVCap concentrations, captured by the UV-Vis-NIR spectrometer with an effective path-length of 5mm.

2.2 Chemometric analysis

Different partial least square (PLS) regression models were developed to predict the concentration of hydrate inhibitors and NaCl in the aqueous solutions. The PLS model can be described as follows:

$$X = TP^T + E \quad (1)$$

$$Y = UQ^T + F \quad (2)$$

Where X is the matrix of spectral data and Y is the matrix of responses; P and Q represents the loading matrix of X and Y respectively. T and U are, respectively, score matrices of X and Y; and E and F are called residuals.

All the references (Empty cuvettes) and sample spectra were first normalised by their respective maximum value and converted to absorbance unit (AU). Different pre-processing methods were applied to the whole spectra before developing the calibration models (i.e., multiplicative scatter correction, standard normal variate, first and second Savitzky-Golay derivatives). Root mean square of cross validation (RMSECV) and root mean square of prediction (RMSEP) were used to evaluate the performance of the developed PLS models and to select the optimum number of the latent variables (LV). RMSECV and RMSEP are calculated according to following equation:

$$RMSE = \sqrt{\frac{\sum_{i=1}^{i=n}(x_i - y_i)^2}{n}} \quad (3)$$

Where x_i and y_i are the reference value and the predicted value by the PLS model respectively; and n is the number of calibration/prediction samples. It should be noted that the Kennard-stone algorithm was utilized to split the data set into calibration and prediction sets and the leave-one-out cross-validation method was employed to develop the PLS models and to select the optimum LV numbers. In this study, the best results in terms of the RMSEP and RMSECV were obtained while the spectra were pre-treated using the first Savitzky-Golay derivative (SGD1 hereafter). In this communication, we thus report results from PLS models that developed utilizing this pre-treatment. Presence of outliers in the calibration dataset was detected by calculating Q residuals and Hotelling's T2 (95% confidence level) during construction of PLS models.[21, 22] To investigate the significance of bias in each PLS model the standard error of prediction (SEP) was calculated.

$$SEP = \sqrt{\frac{\sum_{i=1}^{i=n}(x_i - y_i - bias)^2}{n-1}} \quad (4)$$

$$bias = \frac{\sum_{i=1}^{i=n}(x_i - y_i)}{n} \quad (5)$$

Relative prediction deviation (RPD) was calculated to investigate the practical utility of each model using following equation:

$$RPD = \frac{SD}{SEP} \quad (6)$$

Where SD is the standard deviation of all the predicted data set. More details about the PLS, RMSECV, RMSEP, SEP, bias, RPD and different pre-processing methods can be found in other studies.[23, 24] All the analysis were performed in Unscrambler® X10.3 (CAMO, Oslo, Norway).

Moreover, the limit of detection (LoD) was calculated for all the created calibration models. To calculate the LoD, the spectra of ten samples of water without any solute and the spectra of 10 samples with the highest value of MEG, MeOH, NaCl and PVCap were measured. Then, the final PLS regression model for each component was employed to predict the concentration of the interested component. Then, the average standard deviation of the predicted values was calculated for each model and was multiplied by 10/3 to estimate the LoD [24, 25].

3. EXPERIMENTAL METHOD

3.1 Experimental equipment

A broadband, 20 W tungsten-halogen light source (HL-2000-FHSA, Ocean Optics) and UV/VIS/NIR light source (L10290, Hamamatsu) were guided to an FT-NIR spectrometer (Arcoptix) and UV-VIS-NIR spectrometer (C10082MD, Hamamatsu Ltd.) respectively via a cuvette containing the test sample using fibre optic cables. For NIR analysis, samples were scanned in a cuvette with a pathlength of 1 mm, and internal volume of 350 μL and a cuvette with a pathlength of 5 mm and internal volume 1750 μL was employed for UV analysis. The cuvettes were mounted in a metallic jacket that was temperature controlled by circulating fluid from a circulating water bath. The FT-NIR spectrometer can cover the spectral range of 900 - 2500 nm and the UV-Vis-NIR spectrometer covers the range between 200 to 1100nm. The

absorption of wavelengths across this range is measured relative to a reference spectrum measured with air. The FT-NIR spectrometer has USB connectivity for control and data acquisition.

3.2 Procedure

Before starting each measurement, the cuvette was cleaned using deionized water and acetone, and compressed air was used to dry the cuvette. Then, the sample was loaded into a cuvette and mounted in the metallic jacket. The system was left for 2 minutes to reach thermal equilibrium. For measurements of test samples, an average of twenty spectra was recorded, and the same test sample was measured typically three times using three different aliquots of the sample. The temperature was set to 293.15 K in all measurements. The uncertainty of the measured temperature was U (T) = 0.05 K.

3.3 Materials

Chemicals used in these experiments were MEG and MeOH with 99.5% purity and NaCl salt which was 99.5% pure. All aforementioned chemicals were provided by Sigma Aldrich. PVCap was supplied by BASF. Three comprehensive calibration and prediction data sets were prepared using about 400 solutions covering the concentrations shown in Table 1. All samples were prepared gravimetrically using deionized water to cover the typical concentration ranges of hydrate inhibitors .[8]

Table 1. Concentration ranges for PLS model calibration

Hydrate Inhibitor	Calibration range #1 mass%	Calibrated range #2 mass%	Calibrated range #3 mass%
MEG	0 - 50	-	0 - 50
MeOH	-	0-50	-
PVCap	-	-	0 - 3
NaCl	0 - 7	0 - 7	0 - 7

4. RESULTS AND DISCUSSION

After applying SGD1 with five smoothing points to calibration data set, different PLS models were developed by employing different wavelength regions in the ranges 1400-1850 nm. To examine the performance of the models, three spectral regions were selected for construction of the calibration models: “A” (1400-1850 nm), “B” (1400-1600 nm), “C” (1600-1850). The same regions were also used to determine the concentration of salt according to the changes in absorption of water, MEG and MeOH in the presence of different concentrations of NaCl. Regarding PVCap, the PLS models were developed in the range between 300 and 350 nm. It should be noted that the solutions that were used as the calibration data set contain different concentrations of NaCl and MEG. Therefore, a single wavelength in UV region cannot be used to create a linear regression model for measuring the concentration of PVCap in the solution as the presence of other solutes in the solution affects the accuracy of the linear regression model. The appropriate wavelength region and the best pre-processing method for all the developed models were determined according to the calculated RMSECV, RMSEP and SEP values, and finally, the model which provides the lower prediction errors was select as a final model.

4.1 MEG/Methanol-NaCl systems

The maximum concentration of MEG and MeOH was set to 50 mass% and salt set to 7 mass%. In this study, the spectra were pre-processed using SGD1 with different smoothing points. The best results in terms of RMSECV, RMSEP and SEP values were obtained while the SGD1 with five smoothing points was applied to the dataset. For each MeOH-NaCl and MEG-NaCl systems, 60 samples were used for calibration, and 25 independent samples within the calibration range were used to assess the accuracy of the developed calibration models. The NIR spectra of some of the calibration solutions after SGD1 treatment for MEG/MeOH-NaCl systems are illustrated in Figure 4.

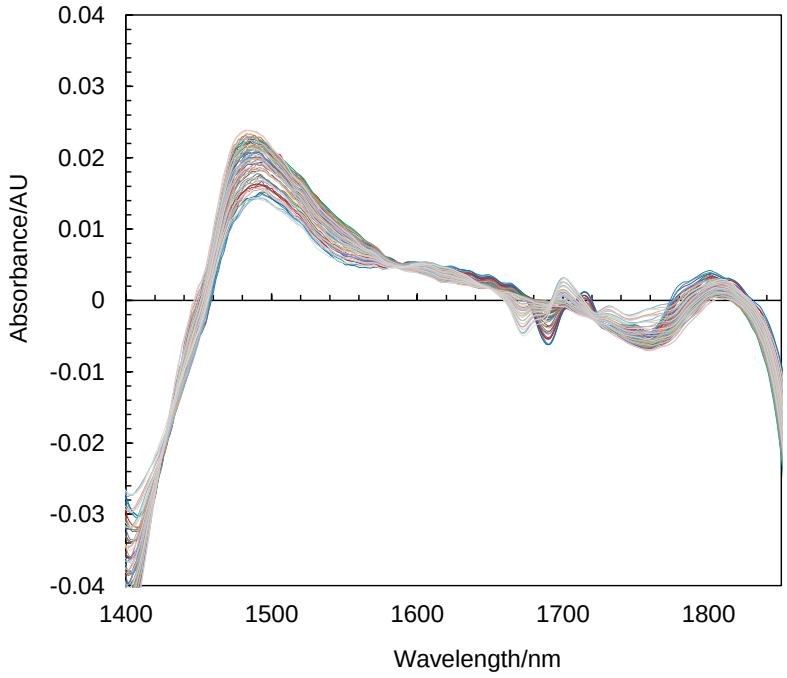

Figure 4. NIR Spectra of various water samples with different MEG, MeOH and salt concentrations after applying the SGD1 pre-treatment (1400 – 1850 nm).

The performance of each PLS model at various spectral ranges is presented graphically through plots of NIR-predicted data obtained from the PLS models versus the measured values. Figures 5 and 6 show that the measured and predicted values of MEG, MeOH and NaCl well agreed.

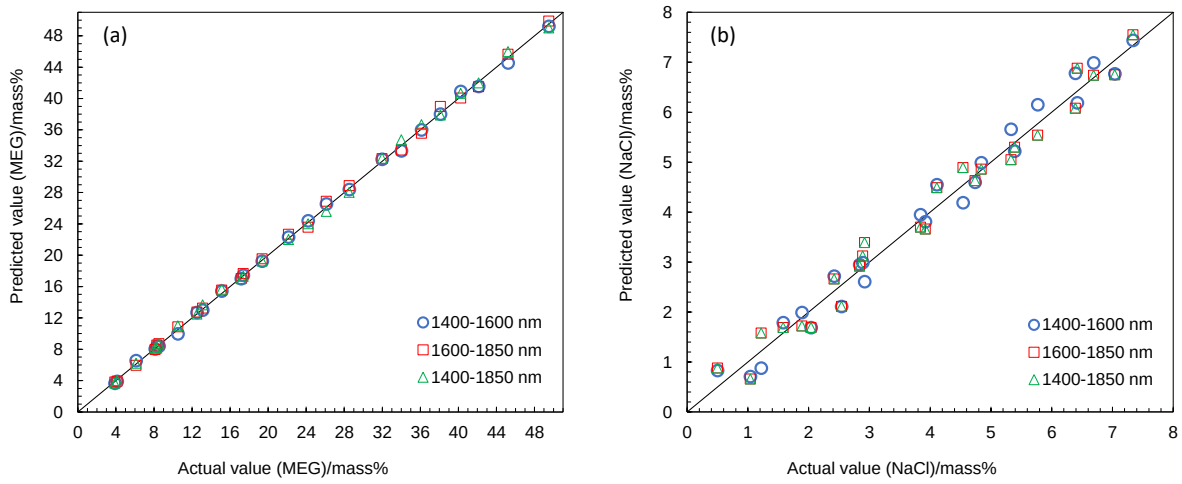

Figure 5. PLS regression plot of predicted versus actual concentration of MEG (a) and NaCl (b) at different wavelength ranges.

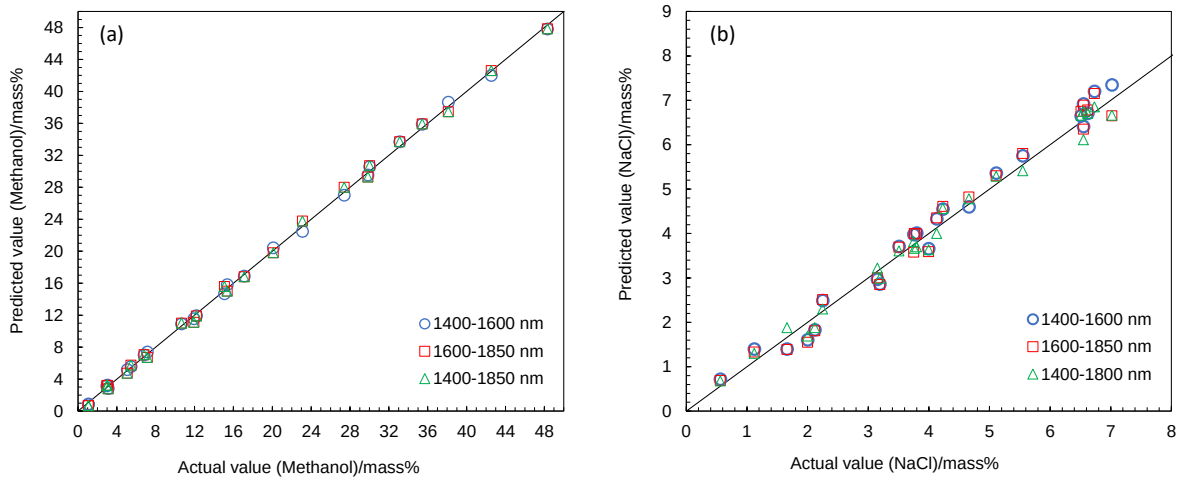

Figure 6. PLS regression plot of predicted versus actual concentration of MeOH (a) and NaCl (b) at different wavelength ranges.

Table 2. Summary of results for calibration and prediction sets.

Inhibitor	Wavelength	LV	RMSECV (mass%)	R^2	RMSEP (mass%)	R^2	Bias (mass%)	SEP (mass%)	RPD	LoD (mass%)
MEG	A(1400-1850)	4	0.147	0.999	0.380	0.999	-0.058	0.201	34.90	0.53
	B(1400-1600)	4	0.141	0.999	0.342	0.999	0.052	0.179	40.35	0.52
	C(1600-1850)	5	0.222	0.999	0.417	0.999	-0.087	0.286	31.64	0.52
NaCl	A(1400-1850)	4	0.133	0.998	0.209	0.997	-0.024	0.142	9.42	0.20
	B(1400-1600)	4	0.219	0.995	0.279	0.994	-0.013	0.255	7.13	0.21
	C(1600-1850)	4	0.228	0.995	0.286	0.995	-0.012	0.251	6.94	0.21
MeOH	A(1400-1850)	4	0.252	0.999	0.378	0.999	0.008	0.386	36.69	0.71
	B(1400-1600)	5	0.306	0.999	0.422	0.999	-0.006	0.431	32.86	0.71
	C(1600-1850)	4	0.309	0.999	0.456	0.999	0.037	0.465	30.49	0.71
NaCl	A(1400-1850)	5	0.159	0.997	0.207	0.997	0.011	0.224	9.74	0.20
	B(1400-1600)	4	0.225	0.997	0.268	0.996	-0.062	0.266	8.20	0.20
	C(1600-1850)	4	0.221	0.995	0.274	0.996	-0.045	0.277	7.90	0.21

Table 2 reports the results obtained for calibration and prediction sets. All of the models performed very well in predicting the concentration of MEG, MeOH and NaCl in water samples not included in the calibration set .The R^2 for predicted samples ranged from 0.994 to 0.999 with SEP ranging from 0.142 to 0.456 mass%, indicating the good predictive ability of all the developed PLS models.

Regarding MEG, the best results in terms of SEP values were found for models that were created in the regions “A” and “B”, slightly larger SEP values in the region “C”, suggesting that the PLS model in region “C” cannot predict the MEG content in solutions containing MEG, water and NaCl as accurate as those in region “A” and “B”. Region “A” is related to the first overtone region of OH bond and first overtone of the C-H stretching for CH_2 bond, whereas the changes in absorption bands in region “B” is attributed to first overtone region of OH bond. It can be seen from Table 2, the developed PLS model for MEG in region “B” shows slightly lower RMSEP and RMSECV values than one created in the region “A”.

For MeOH, Region "A", which corresponds to the first overtone region of OH bond and first overtone region of C-H stretching for CH_3 bond was shown the best results in terms of RMSECV and SEP values.

Regarding NaCl, for both MEG-NaCl and MeOH-NaCl systems, the best results were observed when the wider spectral range ("A") was employed for the construction of the calibration models. The calculated SEP values in region "A" for MEG-NaCl and MeOH-NaCl solutions were 0.142% and 0.224% respectively, for the created NaCl prediction model. In fact, NaCl does not absorb the NIR light, but the presence of the NaCl in the aqueous solution can cause distortion in the regions that water absorbs the NIR light due to a perturbation that sodium and chloride ions create on the hydrogen bond network. All these results demonstrate that NIR spectroscopy technique can predict the concentration of MEG, MeOH and NaCl simultaneously with very good accuracy (High RPD values) in aqueous solutions.

4.2 MEG-PVCap-NaCl systems

Taking account very low concentrations of KHI inhibitors are usually injected at the upstream of the pipelines, some companies are thinking of swapping from thermodynamic hydrate inhibitors such as MEG and MeOH to LDHIs. In the transition procedure, both thermodynamic and kinetic inhibitors are being injected.[26] After injecting both inhibitors for a period of time, they start to decrease the concentration of thermodynamic inhibitors gradually and hence both LDHI and thermodynamic inhibitor will exist in the aqueous solution. Moreover, it is well-known that KHIs can only operate under some level of subcooling. Excess subcooling could lead to the KHI failure to delay nucleation and formation of gas hydrates. Therefore, a combination of a thermodynamic inhibitor with a KHI is accepted as an alternative option. The objective of this section is to investigate the ability of spectroscopy methods for predicting the concentrations of PVCap (KHI) and NaCl in aqueous solutions containing MEG (KHI).

PVCap is a low molecular weight polymer. As polymers strongly absorb UV light, UV was coupled with NIR together to determine the concentration of PVCap, NaCl and MEG simultaneously. For this purpose, all the calibration and prediction samples were analysed using a UV-VIS spectrometer and a NIR spectrometer, and the interested spectral ranges were selected for the construction of the calibration models. The PLS models were developed for solutions containing 0 to 3 mass% PVCap, 0 to 50 mass% MEG and 0 to 7 mass% NaCl. All the measurements were carried out at a temperature of 293.15 K. The presence of PVCap in the solutions did not allow to employ the calibration models that were previously developed for MEG-NaCl systems as NIR spectrum is susceptible to the presence of either impurities or solutes that were not accounted for the construction of the calibration models. 175 samples were prepared as calibration samples, and 55 samples were prepared to assess the performance of the calibration models.Figure 7 illustrates the agreement of the measured MEG, NaCl and PVCap contents with the predicted values in aqueous samples.The UV spectrum between 300 to 350 nm was selected to develop the PLS model for PVCap. It should be mentioned that all the UV spectra were pre-treated by applying SGD1 with 5 moving-point windows (2^{nd} order polynimal). The results obtained for the calibration models for all the components are shown in Table 3. The PLS models for PVCap determination indicated in Table 3 had RMSECV of 0.062 for calibration set and SEP value of 0.096 for prediction sets. The correlation coefficient for the prediction set was 0.997 and was obtained using 4 latent variables, showing the consistency of the developed model. Similar results to those for the MEG-NaCl system were observed for MEG and NaCl while PVCap present in the calibration and prediction solutions.

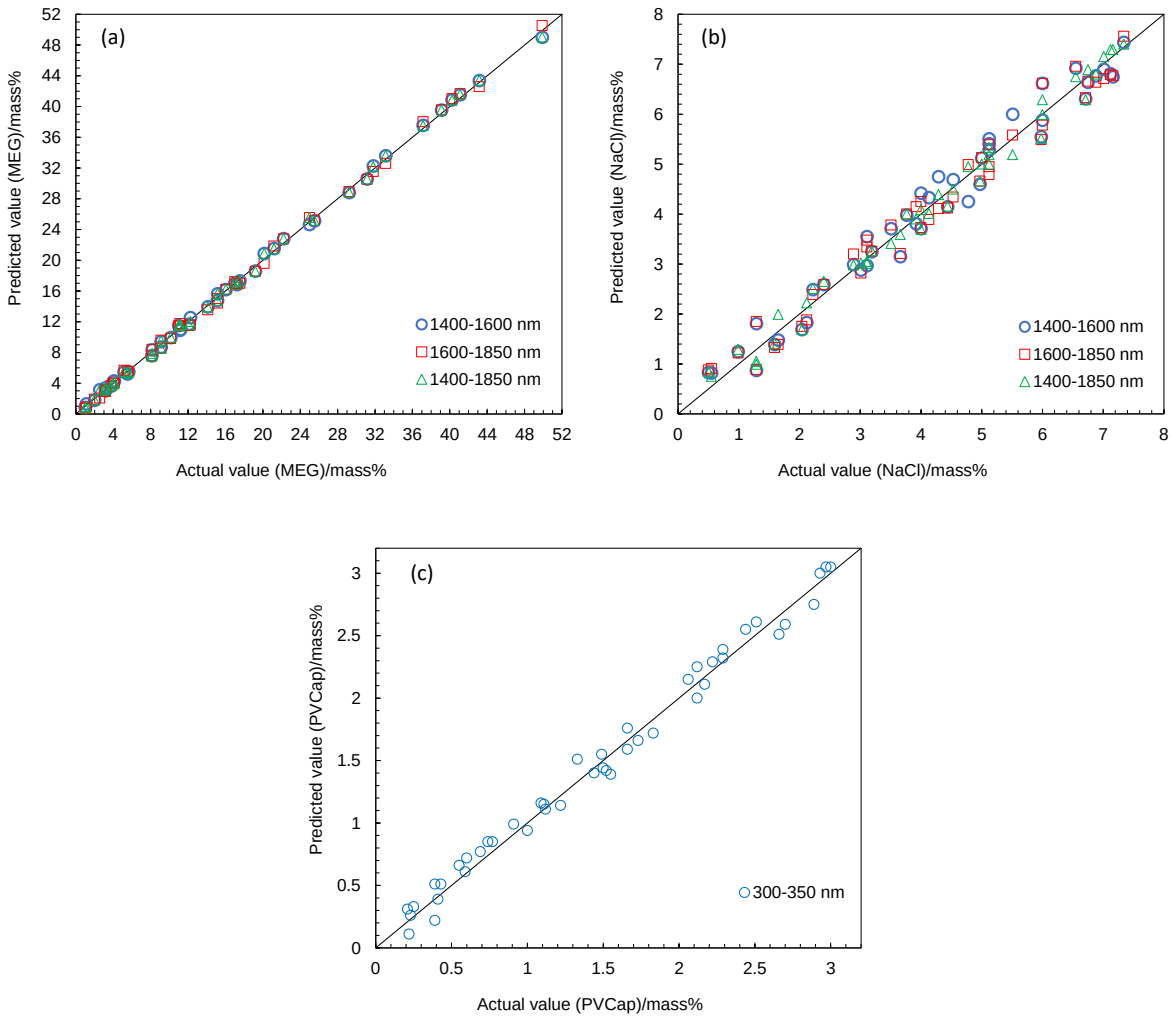

Figure 7. PLS regression plots of predicted versus actual concentration of MEG (a), NaCl (b) and PVCap (c) at different wavelength ranges.

Table 3. Summary of results for calibration and prediction sets

Inhibitor	Wavelength	LV	RMSECV (mass%)	R^2	RMSEP (mass%)	R^2	Bias (mass%)	SEP (mass%)	RPD	LoD (mass%)
MEG	A(1400-1850)	5	0.237	0.999	0.409	0.999	-0.028	0.408	32.06	0.61
	B(1400-1600)	5	0.221	0.999	0.395	0.999	0.024	0.395	33.16	0.62
	C(1600-1850)	5	0.282	0.999	0.475	0.999	0.056	0.472	27.54	0.61
NaCl	A(1400-1850)	5	0.183	0.998	0.215	0.997	-0.007	0.215	9.87	0.24
	B(1400-1600)	5	0.269	0.995	0.319	0.994	-0.011	0.318	6.65	0.24
	C(1600-1850)	5	0.278	0.995	0.302	0.994	0.022	0.301	6.94	0.24
PVCap	300-350	4	0.062	0.997	0.096	0.997	-0.014	0.095	9.198	0.11

4.3 Evaluation of the developed spectroscopic technique

The developed spectroscopic method was evaluated in the presence of gas hydrates in the system, simulating gas hydrate formation in a natural gas transport pipeline. As a typical example, a MEG-NaCl system was used for evaluation. Figure 8 shows the schematic of the setup. A stainless steel autoclave vessel of 2.3 L was used to form gas hydrate. It had a volume of 2.3 L and was equipped with a magnetic stirrer. About 500 ml of aqueous solution containing 6.67 mass% NaCl and 10 mass% MEG was loaded into the autoclave. The system temperature was controlled by a cooling bath that circulates coolant through a cooling jacket surrounding the autoclave. After vacuuming natural gas was injected until the system was pressurised to the desired pressure. The natural gas composition is shown in Table 4. The system was cooled down in steps and left overnight at each test temperature to allow thermodynamic equilibrium. At each equilibrium step, aqueous sample was drained from the bottom of the autoclave, and the light spectra were analysed by the NIR spectrometer. Finally, the concentration MEG and NaCl was determined using the developed PLS models.

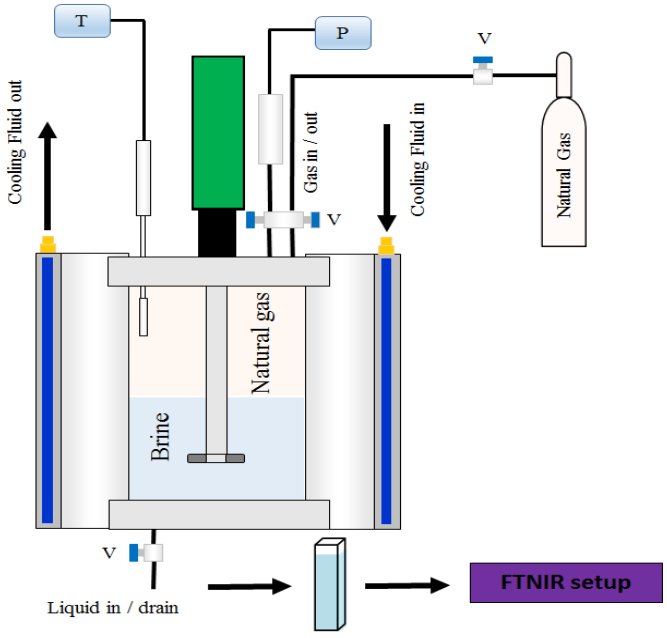

Figure 8. Schematic of the experimental setup

Table 4. Composition of the natural gas

Component	CO_2	N_2	C_1	C_2	C_3	i-C_4	n-C_5	i-C_5	n-C_5
Concentration (mol%)	1.32	1.02	90.29	5.48	1.35	0.20	0.25	0.20	0.10

The first sample was taken when the system was outside hydrate stability zone; then the system was directly cooled down to the target temperature to form gas hydrates. After hydrate formation, the system was heated up to dissociate the hydrates. The hydrate dissociation process was carried out stepwise. The system was kept at each temperature for about 24 hours, and at each temperature, liquid sample was taken from the bottom of the autoclave, which normally resulted in about 0.01 MPa drop in the system pressure. All these liquid samples were placed into a quartz cuvette and analysed using the NIR spectrometer. The created PLS models that were then used to predict the concentration of MEG and NaCl in the aqueous solutions. Figure 9 highlights the sampling points throughout the experiment.

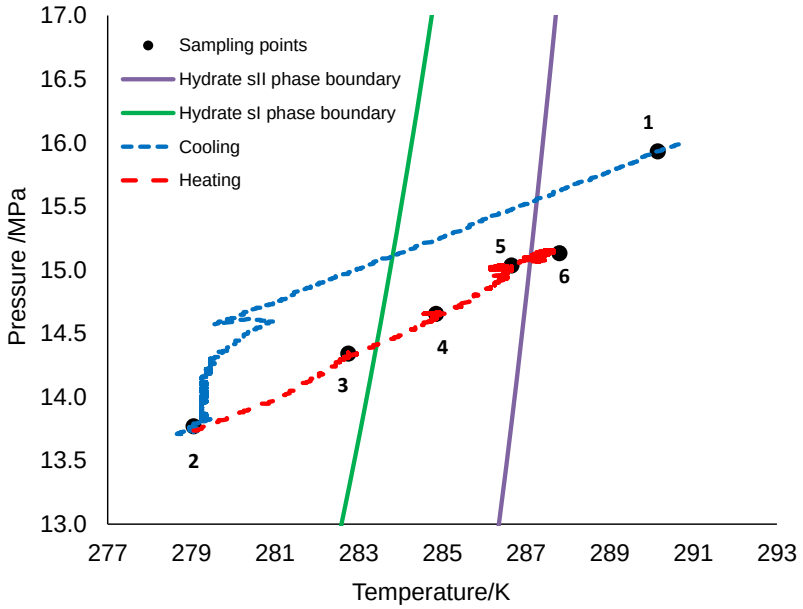

Figure 9. Temperature-pressure profile and sampling points for the system with natural gas, deionized water, MEG and NaCl.

- Sample 1: at 290.15 K and 15.93 MPa outside hydrate stability zone
- Sample 2: at 279.05 K and 13.77 MPa inside the sI and sII hydrate stability zones.
- Sample 3: at 282.75 K and 14.34 MPa inside the sI and sII hydrate stability zones.
- Sample 4: at 284.85 K and 14.65 MPa outside the sI hydrate stability zone and inside sII hydrate stability zone.
- Sample 5: at 286.65 K and 15.03 MPa outside the sI hydrate stability zone and inside sII hydrate stability zone.
- Sample 6: at 287.25 K and 15.13 MPa outside hydrate stability zone.

Table 5 shows the evaluation results. Both salt concentration and MEG concentration were measured using the developed PLS models, which is listed in the column that is marked “NIR”,

while the column “Exp” signifies the experimental concentrations that were calculated based on the original concentration and the reduction of water because of formation of gas hydrates (See Appendix for details). As shown in Table 5, the NIR measured salt (NaCl) concentrations are in good agreement with the actual values, and the deviations are less than 0.2 mass%, indicating the accuracy of the developed method. Hydrates excluded salt from their structures, therefore upon hydrate formation, the concentration of salt in the remaining free water increased after hydrate formation. Furthermore, the increase in the concentration of salt is proportional to the amount water converted into hydrates. Similarly, during the heating steps, water resulting from hydrate dissociation, reduced the salinity. At Stage 1 (before hydrate formation) and Stage 2 to 5 (during hydrate dissociation), the measured MEG concentrations are also in good agreement with the experimental values in about 0.2 mass% of measurement deviation. It should be noted that slightly larger deviation was observed for the last sample. This might be attributed to the fact that tiny amount of gas hydrate still remained in the system at the conditions just outside the hydrate stability zone (Figure 9).

Table 5. Evaluation results of the NIR method

T	P	Water in hydrate	NaCl (mass%)		MEG (mass%)	
K	MPa	Barrel/MMscf	Exp	NIR	Exp	NIR
290.15	15.93	0	6.31	6.67	10.0	10.05
279.05	13.77	115.2	8.72	8.82	12.64	12.56
282.75	14.34	75.50	8.59	8.68	12.58	12.81
284.85	14.65	25.21	8.10	8.17	12.01	12.14
286.65	15.03	7.12	7.81	7.70	11.29	11.14
287.25	15.13	0	6.29	6.71	9.96	10.24

The described system is suited for determining the composition of hydrate inhibitors as well as NaCl. As measurement times in the order of seconds (including data acquisition and

evaluation) can be realised, the system is capable of providing online liquid characterization. Furthermore, this method is more promising in compare with another available method such as GC and densitometer. The presence of inorganic salts worsened the performance of the GC and could even damage the columns of the GC and densitometer is not capable of measuring the concentration of alcohols precisely while the concentration of salt is varying in the system. Both GC and densitometer are not able to predict the concentration of salt in the aqueous solutions. Based on the results obtained in this study the spectroscopy methods are capable of predicting the concentration of NaCl and hydrate inhibitors without any trouble and can be used as a suitable method for monitoring hydrate safety margin with a high level of confidence.

5. CONCLUSIONS

Application of the spectroscopy method was investigated to measure the concentration of hydrate inhibitors and NaCl in three hydrate inhibition systems including MEG-NaCl, MeOH-NaCl, PVCap-NaCl systems. Different PLS models developed utilizing both NIR and UV spectra are capable of predicting the concentration of MEG, MeOH, PVCap, and NaCl in aqueous solutions. In terms of standard error of prediction (SEP), the best results were obtained in the wavelength range between 1400-1850 nm for MeOH ($SEP_{(MeOH)-NaCl} = 0.386$) and NaCl ($SEP_{(MEG)-NaCl} = 0.142$, $SEP_{(MeOH)-NaCl} = 0.224$ and $SEP_{(PVCap)-MEG-NaCl} = 0.215$ mass%) and in the wavelength range between 1400 and 1600 nm for MEG ($SEP_{(MEG)-NaCl} = 0.179$ and $SEP_{(PVCap)-MEG-NaCl} = 0.395$ mass%). Moreover, to determine the concentration of PVCap in the (PVCap)-MEG-NaCl solutions, the UV spectrum between 300-350 nm was found to be the optimal for the construction of PLS models, leading to 0.095 mass% of SEP. For the above-mentioned models, the RPD value for MEG and MeOH was greater than 30 and for PVCap and Nacl was greater than 9, indicating the high accuracy of the developed models.

By means of the integration of NIR and UV spectra, the developed PLS models can accurately determine the concentration of PVCap, MEG, and NaCl in a THI-KHI-salt inhibition system.

ACKNOWLEDGEMENTS

This work is part of the joint industrial project (JIP) at the Institute of Petroleum Engineering, Heriot-Watt University. The JIP was finantially funded by BP and TOTAL, which is acknowledged. The authors would also like to thank Grant Paterson for his fruitful comments and discussions.

APPENDIX

To roughly estimate the amount of water converted to hydrate at different P-T conditions, the pressure drop in the system (ΔP) was calculated at different sampling points, and the hydration number (H_n) is assumed constant and equal to 6.5. Hydration number is the number of water molecules per gas molecule at a given P-T condition. The amount of water converted to hydrate can be estimated using Eq. 7:

$$WCH\% = \frac{\Delta n_{water}}{n_w} \tag{7}$$

$$\Delta n_{gas} = \frac{\Delta P}{P} n_{gas} \tag{8}$$

n_{gas} and P are the number of gas moles in the gas phase and pressure of the system respectively, before the formation of the gas hydrate. The water mole fraction can be determined by:

$$f_w = \frac{n_{water}}{n_{gas} + n_{water}} = \frac{n_{water}}{n_{tot}} \tag{9}$$

The number of water moles used in hydrates (Δn_{water}) is then calculated using equation 11.

$$\Delta n_{gas} = \frac{\Delta P}{P} (1 - f_w) n_{tot} \tag{10}$$

$$\Delta n_{water} = H_n \frac{\Delta P}{P} (1 - f_w) n_{tot} \quad (11)$$

Then, WCH can be estimated using equation 12 in litre:

$$WCH\ \% = H_n \frac{\Delta P}{P} \frac{(1 - f_w)}{f_w} \quad (12)$$

In this study, the amount of water converted to hydrate is expressed in bbl/MMscf unit. For this purpose, the amount of water converted in hydrate in gram is calculated by multiplying Δn_{water} by 18.01 gr/mol and converted to litre unit (the density of water is assumed to be 1000 gr/L). The amount of water is then converted to U.S. barrel (bbl) by multiplying by 0.0086 and the volume of the gas in litre is estimated ($V = ngasZRT/P$, assuming standard condition T = 288.70K and P = 0.1 MPa) and converted to million standard cubic feet (MMscf is a volume unit in the petroleum industry.) by multiplying by 0.0035.

REFERENCES

(1) Tohidi, B.; Anderson, R.; Chapoy, A.; Yang, J.; Burgass, R. W. Do we have new solutions to the old problem of gas hydrates? *Energy & Fuels* **2012,** 26, (7), 4053-4058.

(2) Hammerschmidt, E. Formation of gas hydrates in natural gas transmission lines. *Industrial & Engineering Chemistry* **1934,** 26, (8), 851-855.

(3) Zhao, H.; Sun, M.; Firoozabadi, A. Anti-agglomeration of natural gas hydrates in liquid condensate and crude oil at constant pressure conditions. *Fuel* **2016,** 180, 187-193.

(4) Yang, J.; Chapoy, A.; Mazloum, S.; Tohidi, B. Development of a Hydrate Inhibition Monitoring System by Integration of Acoustic Velocity and Electrical Conductivity Measurements. *Exploration and Production: the Oil and Gas Review* **2011,** 9, (1), 36-40.

(5) Yang, J.; Chapoy, A.; Mazloum, S.; Tohidi, B. A novel technique for monitoring hydrate safety margin. *SPE Production & Operations* **2012,** 27, (04), 376-381.

(6) Henning, B.; Daur, P.-C.; Prange, S.; Dierks, K.; Hauptmann, P. In-line concentration measurement in complex liquids using ultrasonic sensors. *Ultrasonics* **2000,** 38, (1), 799-803.

(7) Sandengen, K.; Kaasa, B. Estimation of monoethylene glycol (MEG) content in water+ MEG+ NaCl+ NaHCO3 solutions. *Journal of Chemical & Engineering Data* **2006,** 51, (2), 443-447.

(8) Yang, J.; Tohidi, B. Determination of hydrate inhibitor concentrations by measuring electrical conductivity and acoustic velocity. *Energy & Fuels* **2013,** 27, (2), 736-742.

(9) Gowen, A.; Marini, F.; Tsuchisaka, Y.; De Luca, S.; Bevilacqua, M.; O'Donnell, C.; Downey, G.; Tsenkova, R. On the feasibility of near infrared spectroscopy to detect contaminants in water using single salt solutions as model systems. *Talanta* **2015,** 131, 609-618.

(10) Lin, J.; Brown, C. W. Near-IR spectroscopic measurement of seawater salinity. *Environmental science & technology* **1993,** 27, (8), 1611-1615.

(11) Grant, A.; Davies, A. M.; Bilverstone, T. Simultaneous determination of sodium hydroxide, sodium carbonate and sodium chloride concentrations in aqueous solutions by near-infrared spectrometry. *Analyst* **1989,** 114, (7), 819-822.
(12) Fernandes, H. L.; Raimundo Jr, I. M.; Pasquini, C.; Rohwedder, J. J. Simultaneous determination of methanol and ethanol in gasoline using NIR spectroscopy: effect of gasoline composition. *Talanta* **2008,** 75, (3), 804-810.
(13) Guo, Q.; Small, G. W. Quantitative determination of methanol and ethanol with synthetic calibration spectra in passive Fourier transform infrared remote sensing measurements. *Applied spectroscopy* **2013,** 67, (8), 913-923.
(14) Ouyang, A.; Liu, J. Classification and determination of alcohol in gasoline using NIR spectroscopy and the successive projections algorithm for variable selection. *Measurement Science and Technology* **2013,** 24, (2), 025502.
(15) Anderson, R.; Tohidi, F.; Mozaffar, H.; Tohidi, B. KINETIC HYDRATE INHIBITOR REMOVAL FROM PRODUCED WATERS BY SOLVENT EXTRACTION. *Journal of Petroleum Science and Engineering* **2016**.
(16) Gibbons, M. K.; Örmeci, B. Quantification of polymer concentration in water using UV-Vis spectroscopy. *Journal of Water Supply: Research and Technology-Aqua* **2013,** 62, (4), 205-213.
(17) Tohidi, B.; Anderson, R.; Mozaffar, H.; Tohidi, F. The return of kinetic hydrate inhibitors. *Energy & Fuels* **2015,** 29, (12), 8254-8260.
(18) Mozaffar, H.; Anderson, R.; Tohidi, B. Effect of alcohols and diols on PVCap-induced hydrate crystal growth patterns in methane systems. *Fluid Phase Equilibria* **2016,** 425, 1-8.
(19) Tohidikaloorazy, F. Fundamental controls on kinetic hydrate inhibitor performance and polymer removal from produced waters. Heriot-Watt University, 2016.
(20) Cha, M.; Shin, K.; Kim, J.; Chang, D.; Seo, Y.; Lee, H.; Kang, S.-P. Thermodynamic and kinetic hydrate inhibition performance of aqueous ethylene glycol solutions for natural gas. *Chemical Engineering Science* **2013,** 99, 184-190.
(21) Bro, R.; Smilde, A. K. Principal component analysis. *Analytical Methods* **2014,** 6, (9), 2812-2831.
(22) Ballabio, D.; Consonni, V. Classification tools in chemistry. Part 1: linear models. PLS-DA. *Analytical Methods* **2013,** 5, (16), 3790-3798.
(23) Rinnan, Å.; van den Berg, F.; Engelsen, S. B. Review of the most common pre-processing techniques for near-infrared spectra. *TrAC Trends in Analytical Chemistry* **2009,** 28, (10), 1201-1222.
(24) Haghi, R. K.; Yang, J.; Tohidi, B. Fourier Transform Near-Infrared (FTNIR) Spectroscopy and Partial Least-Squares (PLS) Algorithm for Monitoring Compositional Changes in Hydrocarbon Gases under In Situ Pressure. *Energy & Fuels* **2017,** 31, (9), 10245-10259.
(25) Lutz, O. M.; Bonn, G. K.; Rode, B. M.; Huck, C. W. Reproducible quantification of ethanol in gasoline via a customized mobile near-infrared spectrometer. *Analytica chimica acta* **2014,** 826, 61-68.
(26) Vajari, S. M. Development of hydrate inhibition monitoring and initial formation detection techniques. Heriot-Watt University, 2012.

Table of Contents Graphic